ROYAL SOCIETY OF CHEMISTRY

PAPER

Check for updates

Degradation investigation and active packaging performance of cross-linked chitosan film containing gallic acid†

Jessica R. Westlake,[a] Edward Chaloner,[c] Maisem Laabei,[d] Fotis Sgouridis, [e]
Andrew D. Burrows [b] and Ming Xie [*a]

We report the fabrication and analysis of a vanillin cross-linked chitosan film containing gallic acid as the active component. The active packaging material was found to successfully block 100% of UV light and had good water vapour barrier properties. Cross-linking *via* Schiff base formation reduced the water solubility and moisture content of the chitosan films and improved tensile properties, with a force at break measured as 29.4 ± 0.5 N. The material performed well in thermal testing, and we evaluated a glass transition temperature of 274.0 °C. We determined the successful controlled release of gallic acid from the composite film using UV-visible spectroscopy over 2 weeks. The material had strong antioxidant and antimicrobial capacities, reducing >98% of 2,2-diphenyl-1-picrylhydrazyl radicals and inhibiting the growth of both *E. coli* and *S. aureus*. We investigated the degradation of this biopolymer film in different environments including soil, compost, seawater, UV-light and water. The material reached over 90% degradation in soil within 12 weeks, rising to complete degradation after 24 weeks. We also investigated the potential mechanism for the degradation of the chitosan films, showing the effect of moisture and microbial availability in soil, and the related cleavage of the chitosan backbone *via* fragmentation. We determined improved degradation when the active components were released into solution before testing. Overall, the film has good physiochemical properties, strong antioxidant and antimicrobial activity and excellent degradation properties. Thus, the presented material is a strong candidate for future development of sustainable active packaging materials.

Sustainability spotlight

To realise the goal reducing plastic pollution and the use of fossil-fuel based materials, next-generation materials derived from natural resources are a vital development. Waste-valorisation is an increasingly popular area of research, adhering to Sustainable Development Goal (SDG) 12 – focusing on sustainable consumption and production patterns. Satisfying these requirements, chitosan is derived from chitin extracted from crustacean shells as a byproduct of the seafood industry. The use of this biopolymer also aligns with SDG 14 – focusing on the sustainable use of marine resources. Our interest with this material focuses on active packaging, combining chitosan with natural antimicrobial extracts to reduce food spoilage, greenhouse gas (GHG) emissions released by food waste, and the occurrence of foodborne diseases.

1. Introduction

Bio-based polymers, made partly or entirely from renewable natural materials, address environmental concerns by reducing reliance on fossil fuels. The majority (53%) of the current bioplastics market is made up of flexible materials, including food packaging.[1] To compete on performance with conventional plastics, these alternative materials must have good mechanical properties and protect food from water vapour, UV light and microbial contamination. Bio-based active packaging, specifically, functions to reduce food waste by prolonging the shelf-life of food *via* the release of antimicrobial and antioxidant compounds or the sequestration of degradation-enhancing gases. Therefore, these materials aim to increase the sustainability profile of food packaging whilst simultaneously ensuring the safety of food.

Chitosan is the second most abundant biopolymer after cellulose; it is non-toxic, antimicrobial and is approved as a food ingredient by the Food and Drug Administration (FDA). Therefore, composite materials of chitosan are promising for

[a]Department of Chemical Engineering, University of Bath, Bath, BA2 7AY, UK. E-mail: mx406@bath.ac.uk

[b]Department of Chemistry, University of Bath, Bath, BA2 7AY, UK

[c]Department of Biology, University of Bath, Bath, BA2 7AY, UK

[d]School of Cellular and Molecular Medicine, University of Bristol, Bristol, BS8 1TH, UK

[e]School of Geographical Sciences, University of Bristol, Bristol, BS8 1QU, UK

† Electronic supplementary information (ESI) available. See DOI: https://doi.org/10.1039/d5su00229j

packaging development. Chitosan is produced by the deacetylation of chitin, which is extracted from crustacean shells, fungi cell walls or insect exoskeletons. Between 15 and 40% of the composition of crustacean shells is chitin, and other parts including minerals and proteins can be valorised as animal feed, pigments and food supplements.[2,3] When waste crustacean shells from the seafood industry are used as the source for chitosan, this can be considered as marine biomass valorisation.[4] Indeed, crustacean shells are the source used for the industrial-scale production of chitosan.[5]

Research on optimising the extraction process of chitosan is prevalent in the literature due to the current associated costs acting as a barrier to larger scale commercialisation of chitosan-based packaging materials. Furthermore, research is being carried out on optimising the sustainability of the extraction process, adhering to the principles of green chemistry.[6] Rocha-Pimienta et al. recently described their optimisation of chitosan extraction from fishery waste, achieving over 20% yield of chitosan and concluding that their method could be implemented in industry to reduce costs.[2] Furthermore, Suresh et al. utilised a proteolytic bacterium Stenotrophomonas koreensis to extract chitin from fish scale waste with a yield of 28%.[7] Overall, the implementation of a marine biorefinery with improved yields and 'green' chemical strategies, in accordance with the United Nations Sustainable Development Goals, will allow for larger scale commercialisation of chitosan-based materials.[4]

Natural chitosan biopolymer has a high tendency for hydrogel formation and so cross-linking is often used to reduce water-sensitivity and swelling, whilst improving mechanical and barrier properties.[8] Cross-linking can also optimise the controlled release of active compounds from within the polymer matrix by reducing diffusion pathway lengths. Previously, chemicals such as formaldehyde and glutaraldehyde have been used to cross-link chitosan. However, more recently there has been a movement towards the use of naturally derived, 'green' cross-linkers. Citric acid is commonly used in this context and has been demonstrated to improve water resistance, thermal stability, mechanical strength and barrier properties of chitosan films.[5,9] Quercetin, which can be extracted from onion waste, has also been utilised as a cross-linker for the release of antimicrobial drug compounds in a biomedical setting.[10] Furthermore, Tomadoni et al. utilised response surface methodology to determine the optimal film formation content of vanillin as a cross linker for potential use as a food packaging material.[11] Another study by Zhang et al. reported the enhancement of mechanical properties of chitosan via vanillin mediated cross-linking, with a content of 0.5–10% vanillin.[12] The group reported an increase in tensile strength of over 50% and a reduction in water vapour permeability.[12] Although cross-linking has been used repeatedly as a technique to elicit controlled release in the literature, this is more common in a biomedical context, with fewer studies incorporating this technology for active packaging. Overall, cross-linking can be utilised to optimise the properties of chitosan films for active food packaging materials.

Potent antioxidant and antimicrobial properties are vital for successful active packaging materials, reducing food spoilage via lipid oxidation and microbial contamination. Green tea extract contains gallic acid, epigallocatechin gallate and 7 other major catechins, which are responsible for its antioxidant and antimicrobial properties. Green tea extract is inexpensive and readily available with many low-intensity extraction methods.[13] For this reason, it has been widely used in recent active packaging literature, in combination with many polymers including chitosan, and materials have been evaluated on different foodstuffs.[14–17] Gallic acid is a phenolic component of green tea extract and is naturally occurring in many foods and other plant-based sources. Gallic acid has potent antioxidant, antimicrobial and antifungal properties and so holds strong potential for food preservation in sustainable packaging materials.[18] Moreover, incorporating gallic acid can improve other properties including mechanical strength, permeability and UV barrier properties.[18] Therefore, gallic acid can be considered as a safe, natural and potent antimicrobial compound with strong potential when combined with polymers to form active packaging materials.

Many polymers are termed as biodegradable in the literature. However, the degradation rate and capacity vary greatly between different polymers and degradation environments. Biodegradable plastics break down into natural substances through the action of microorganisms, though definitions, conditions and timeframes are often not comparable between different studies. In Europe, for a plastic to be certified as 'compostable', a subset of biodegradable plastics, 90% of the material must breakdown into pieces smaller than 2 mm size in 12 weeks compost environment. Recent policy- and public-driven initiatives have heightened the need to scale-up sustainable packaging materials with the ability to preserve perishable foods and degrade within a suitable timeframe.[19] To this end, degradable active packaging materials aim to address the environmental concerns with plastic waste as water and land pollution, arising from food-contaminated plastics and thin film plastics which are not easily recyclable. Chitosan is a natural polymer and therefore has a chemical structure which can be broken down by enzymes such as lysozymes, which are ubiquitous in nature.[5] Chitosan has a good biodegradation capacity, indeed De Carli et al. reported the fast degradation of chitosan–propolis extract films in soil, reporting complete dissolution after 15 days.[20]

The aim of this study was to elucidate the degradation performance of cross-linked chitosan–gallic acid films in different environments. The biopolymer composite material was tested using a suite of analytical characterisation techniques including the evaluation of tensile properties, barrier properties, antimicrobial properties and an investigation into the controlled release of gallic acid. Overall, our results show that this material is an effective degradable, active packaging material with potential for further development.

2. Materials and methods

2.1. Chemicals

High-molecular weight (HM$_W$) chitosan sourced from crustacean shells (310–375 kDa, >75% degree of deacetylation), vanillin, gallic acid, 2,2-diphenyl-1-picrylhydrazyl (DPPH)

radical, glycerol and ethanol were purchased from Sigma-Aldrich. Reagent-grade glacial acetic acid was obtained from Alfa Aesar. Unless otherwise specified, deionised water was used to prepare all aqueous solutions.

2.2. Preparation of active films

The synthetic method was adapted from a method described in our previous report.[21] 3% (w/v) HM_W chitosan was dissolved in 1% (v/v) aq. acetic acid at room temperature (RT) under magnetic stirring with 50% (w/w) glycerol and 37.5% (w/w) vanillin. After 18 h, 20% (w/w) gallic acid was added in ethanol (<5 mL). After 3 h, the solution was filtered through a 30 µm nylon net filter (Merck Millipore) under vacuum to remove impurities. The solution was then degassed and cast onto a glass plate. The film was left to evaporate solvent for 48 h at RT to afford a transparent yellow film which was denoted as CVGGA.

2.3. Characterisation of films

Prior to any characterization and between analyses, all films were equilibrated in a desiccator at 25% RH and 25 ± 1 °C. At least three samples of the film were prepared, and selected analyses were carried out on films from different experimental series. Laboratory conditions were 25 ± 1 °C and 35% RH. The thickness of each film was measured using a digital micrometer (Fowler Precision) with a precision of ±0.5 µm. An average was calculated using eight measurements of thickness, and the standard deviation of each value was calculated.

2.4. Fourier transform infrared (FTIR) spectroscopy

A Bruker Invenio S Fourier transform infrared spectrometer was used to record the spectra of the dried films and individual film components. The spectral resolution was 4 cm^{-1}, and 40 scans were acquired for each spectrum (4000–400 cm^{-1}). The FTIR spectra of the samples were acquired directly.

2.5. Film microstructure

The film microstructure was characterized using field emission scanning electron microscopy (Jeol 7900, Japan) with 5 kV acceleration voltage under high vacuum. The samples were mounted on aluminium stubs with double-sided carbon tape, placed into a vacuum chamber for 18 h and sputter coated with 10 nm of chromium before imaging. Cross-sectional images were obtained by freeze-fracturing samples in liquid nitrogen prior to mounting. Magnification levels used ranged from 1000 to 100 000×.

2.6. Colour measurements

A colourimeter (Fru WR-10QC) was used to measure the L^* (lightness/darkness), a^* (redness/greenness), and b^* (yellowness/blueness) values of the surface of chitosan films over time. Each film was measured at a minimum of five stochastic points to calculate the average and standard deviation and measurements were taken using a white paper background. Between measurements, samples were left uncovered

in an open-air environment. The yellowness index (YI) was calculated using the following equation:

$$YI = \frac{142.86 \times b^*}{L^*} \tag{1}$$

2.7. Opacity

The absorbance of the films was measured at 600 nm using a Cary-100 UV-visible spectrometer (Agilent Technologies) with an empty quartz cuvette run as a control. The absorbance of the quartz cuvette was deleted from the final absorbance value. The opacity of chitosan films was then calculated using the following equation:

$$Opacity = \frac{absorbance\ at\ 600\ nm(AU)}{film\ thickness(mm)} \tag{2}$$

2.8. UV blocking

The transmittance of chitosan films was measured between 200 and 800 nm using a Cary-100 UV-visible spectrometer (Agilent Technologies). An empty quartz cuvette was run as a control.

2.9. Differential scanning calorimetry (DSC)

DSC analysis was performed using a DSC Q20 build 124 (TA Technologies, USA). Samples were heated at a rate of 10 °C min^{-1} from 25 °C to 300 °C under a nitrogen atmosphere at a flow rate of 20 mL min^{-1}.

2.10. Thermogravimetric analysis (TGA)

TGA measurements were carried out on a Setsys Evolution TGA 16/18 thermogravimetric analyser (Setaram, Switzerland). Thermal degradation was performed in an atmosphere of argon up to 600 °C with a heating ramp of 10 °C min^{-1}. Samples of 10–15 mg were used. Weight loss calculations were carried out for each step of degradation, and the moisture content was evaluated from the mass loss *via* moisture evaporation at 105 °C.

2.11. Mechanical properties

A texture analyzer (INSTRON 3369) with a 100 N load cell was used to measure the tensile properties of chitosan films according to the ASTM D882 method.[22] Pneumatic grips were used to clamp the films using a pressure of 4 bar. The initial grip separation and velocity were adjusted to 100 mm and 12.5 mm min^{-1}, respectively. The values of force and distance were recorded during the extension of the biopolymer film strips. 5 samples of each film were analysed to calculate the average and standard deviation. The elongation at break, tensile strength, Young's modulus, and force at break values were determined for each sample. The thickness for samples was determined as 68 ± 2.7 µm.

2.12. Moisture content and water solubility

Squares of film samples in triplicate were weighed (m_0) and dried in an air circulating oven (Lincat, U.K.) at 105 ± 2 °C until they reached a constant weight (m_1). The dried samples were immersed in 20 mL deionised water for 24 h. The samples were dried in the oven at 105 ± 2 °C for 2 h and reweighed (m_2). The moisture content and water solubility of the films were calculated according to the following equations:

$$\text{Moisture content(\%)} = \frac{m_0 - m_1}{m_0} \times 100 \qquad (3)$$

$$\text{Water solubility(\%)} = \frac{m_1 - m_2}{m_1} \times 100 \qquad (4)$$

2.13. Water contact angle measurements (θ)

Water contact angle measurements were carried out using the sessile drop method in air at RT. Droplets of distilled water (5 μL) were dispensed with a precision syringe onto the horizontal film surface using an OCA 25 instrument (DataPhysics, Germany). Still images were obtained, and the water contact angle was recorded immediately and in triplicate using SCA 20 module base software.

2.14. Water vapour permeability (WVP)

The WVP of chitosan films was determined using a gravimetric method.[23,24] A permeability cup (Elcometer 5100 Payne Cup: 30 × 30 cm) was filled with water, leaving >5 mm of headspace. The film sample was placed on top and secured with a watertight ring and screws. The cup was placed in a desiccator containing silica beads to maintain a low humidity environment. The mass loss of the cup was recorded using an analytical mass balance at regular intervals over 72 h, alongside recordings of the temperature and relative humidity (RH). Slopes of the weight loss *versus* time curves for CVG and CVGGA films were determined *via* linear regression ($R^2 > 0.98$) (Fig. SI, ESI†). The water vapour transmission rate (WVTR), water vapour permeance, and WVP were calculated according to eqn (5)–(7) respectively.[25] The set-up for WVP measurements can be found in the ESI (Fig. S2).†

$$\text{WVTR}\left(\text{g s}^{-1} \text{ m}^{-2}\right) = \frac{\Delta w(\text{g})}{\Delta t(\text{s}) \times A(\text{m}^2)} \qquad (5)$$

$$\text{Permeance}\left(\text{g s}^{-1} \text{ m}^{-2} \text{ Pa}^{-1}\right) = \frac{\text{WVTR}}{\Delta P(\text{Pa})} \qquad (6)$$

$$\text{WVP}\left(\text{g s}^{-1} \text{ m}^{-1} \text{ Pa}^{-1}\right) = \text{permeance} \times \text{thickness(m)} \qquad (7)$$

where $\Delta w / \Delta t$ is the flux measured as mass loss of the cell per unit time, m^2 is the actual exposed area determined by the mouth cup diameter, A is the area of the film exposed to water and ΔP is the water vapour pressure difference across the film, based on the average test temperature and RH, assuming a full water vapour saturation in the headspace.[25,26]

2.15. Release kinetics and migration

A method adapted from our previous research was used to measure the release of gallic acid from chitosan films.[21] Film samples were cut and weighed (79 ± 7 mg) before being submerged in 20 mL of food simulant (95% (v/v) ethanol in water) in closed containers. A Cary-100 UV-vis spectrometer (Agilent Technologies) was used to determine the concentration of gallic acid (measured at 274 nm) released into an aliquot of food simulant at regular time intervals up to 312 hours. After each reading, the film was removed from the simulant and placed into the same volume of fresh simulant to allow for a cumulative reading. All readings were taken in triplicate. Calibration curves were recorded and used to calculate the amount of gallic acid and vanillin released over time (Fig. S3, ESI†). The migration of gallic acid from CVGGA films was measured using UV-visible spectroscopy. Films (50 ± 5 mg) were submerged in 10 mL of a food simulant (deionised water, 50% (v/v) ethanol–water or 95% (v/v) ethanol–water) for 288 h before measurement at 274 nm.

The release kinetics of gallic acid from the chitosan–vanillin matrix were fit to zero- and first-order kinetics (eqn (8) and (9)). The kinetics were better described using the Korsmeyer–Peppas model (eqn (10)) the Higuchi model (eqn (11)) and the approximation derived from Fick's second law (eqn (12)). For both eqn (10) and (12), the approximation can only be used for values of $M_t/M_\infty \leq 2/3$. For eqn (12), the plot of M_t/M_∞ *versus* $t^{1/2}$ results in a linear curve with slope k (eqn (11)).[27–29] The diffusion coefficient (D) for burst release was calculated by rearranging eqn (13). The kinetic constants were determined in each case, and the R^2 values of each mathematical fitting were compared.

$$M_t - M_0 = kt \qquad (8)$$

$$\log M_t = \log M_0 - \frac{kt}{2.303} \qquad (9)$$

$$\frac{M_t}{M_0} = K_{\text{KP}} t^n \qquad (10)$$

$$\frac{M_t}{M_0} = K_{\text{H}} t^{1/2} \qquad (11)$$

$$\frac{M_t}{M_\infty} = \frac{4}{L}\left(\frac{D \times t}{\pi}\right)^{1/2} \qquad (12)$$

$$k = \frac{4}{L}\left(\frac{D}{\pi}\right)^{1/2} \qquad (13)$$

where M_t is the mass of the active compound at time t in hours, M_∞ is the mass at $t = \infty$, k is the kinetic constant for zero- or first-order kinetics, K_{KP} is the kinetic constant for the Korsmeyer–Peppas (KP) model, n is the diffusion or release exponent for the KP model, M_t/M_∞ is the fraction of drug released at time t, K_{H} is the Higuchi kinetic constant, L is the thickness of the film in cm, and D is the diffusion coefficient in $m^2 \text{ s}^{-1}$.

2.16. Antioxidant and antimicrobial properties

2.16.1. Antioxidant activity (DPPH). The antioxidant activity of chitosan films was evaluated using the 2,2-diphenyl-1-

picrylhydrazyl (DPPH) radical method.[30] Films were cut to approximately 3×3 cm (161 ± 8 mg), submerged in 10 mL ethanolic DPPH solution (0.784 mg mL^{-1}) and shaken. The absorbance was measured after 30 min at 517 nm using a Cary-100 UV-visible spectrometer (Agilent Technologies). The absorbance of the diluted DPPH solution without the films was measured as a control. The radical scavenging activity was expressed as a percentage of DPPH quenching using the following equation:

$$\% \ \text{In} = \frac{A_0 - A_s}{A_0} \times 100 \tag{14}$$

where % In is the percentage of DPPH radical inhibition, A_0 is the absorbance of the blank sample, and A_s is the absorbance of the sample.

2.16.2. Bacterial growth conditions and assessment of antimicrobial activity. *Staphylococcus aureus* strain SH1000 was incubated on tryptic soy agar at 37 °C for 18 h. *Escherichia coli* strain DC10B was grown on Luria–Bertani agar at 37 °C for 18 h. Compounds of interest were tested for antimicrobial activity with zones of inhibition (ZOI) and minimum inhibitory concentrations (MIC) determined *via* agar diffusion and broth microdilution according to viscosity and adapted from Clinical and Laboratory Standards Institute methods.[31] In summary, bacterial cultures were separately inoculated in 2 mL Mueller–Hinton broth (MHB) and incubated shaking at 180 rpm at 37 °C for 18 h. Overnight cultures were sub-cultured in MHB and grown to exponential phase by shaking at 180 rpm at 37 °C till they reached an absorbance (OD_{600} nm) of 0.5–0.6.

For determination of ZOI, Mueller–Hinton agar plates were spread with approximately 5×10^5 CFU mL^{-1} from aliquots of 0.5 McFarland standardised inoculum to generate bacterial lawn plates. Samples were plated at a uniform concentration of 30 mg mL^{-1} either being aliquoted (50 μL) onto 6 mm diffusion disks or in membrane preparations and incubated at 37 °C for 18 h. ZOI were measured to ascertain antimicrobial activity. For determination of MIC, bacterial sub-cultures were diluted in MHB to an OD_{600} nm of 0.01 and added to a 96-well round bottom microtiter plate. Samples were added to cultures creating a concentration gradient along the plate with a final concentration range of 0–30 mg mL^{-1}. Plates were incubated at 37 °C for 18 h, before calculating MIC values.

2.17. Degradation studies

2.17.1. Film degradation. Film samples were weighed to determine their initial mass before burying or submerging in different degradation environments. In the laboratory, samples were tested for their degradation in (i) soil obtained from the University of Bath campus held within a container, (ii) seawater (150 mL) collected from Devon, U.K., (iii) autoclaved (Priorclave PS/RSV/EH350) soil from the University of Bath campus and (iv) deionised water (150 mL). Film samples were also submerged in 50 mL of 95% (v/v) ethanol–water simulant for 24 h and rinsed with deionised water before degradation studies in soil as a comparison. Outside, films were tested for their degradation in a home compost bin (Blackwall 220 L Black Compost Converter, Get Composting) filled with compost (Miracle-Gro Peat Free All-

Purpose Compost), soil from the University of Bath, fruit and vegetable waste, leaves and manure (Westland Farmyard Manure). The temperature of the compost bin was measured using a temperature probe (WVR) at 7.1–32.3 °C. The samples were also tested outside between May and August (2024, Bath) for their UV degradation in sunlight. In each instance, the film samples were buried >2 cm below the soil or compost surface. Images of the degradation set-ups can be found in the ESI (Fig. S4).† The studies follow the procedure reported in our previous work, laboratory degradation samples were stored at RT in an open-air environment and for all degradation experiments, masses were taken at various intervals of degradation, usually 4, 8, and 12 weeks.[21] Prior to weighing, degraded samples were briefly rinsed with deionised water and dried in an air-circulating oven (Lincat, U.K.) at 65 ± 5 °C for 1 hour. In each case, the moisture content of the polymer film was considered when calculating percentage mass loss during degradation studies. All experiments were carried out at ambient temperature and aerobic conditions were maintained using regular mixing of soil samples. The pH values for seawater and soil were determined using a pH meter (HACH HQ40d multi meter).

2.17.2. TGA-MS. TGA-MS measurements were carried out from 25–600 °C under an atmosphere of nitrogen at a temperature ramp of 10 °C min^{-1} using a TA Instruments STD 650 machine. A Hidden HPR20 was used to provide evolved gas analysis (EGA) using mass spectroscopy, with a mass range of 1–250 amu. The large peak observed in the data at 28 m/z is due to the N_2 purge gas. EGA values were normalised against results for an empty furnace for pyrolysis data.

2.17.3. DSC-UV. DSC-UV measurements were carried out isothermally at room temperature for 120 minutes under a UV lamp (wavelength range = 320–500 nm, intensity range 20–100 mW cm^{-2}) using a TA Instruments Discovery DSC 250 machine. An atmosphere of compressed dry air was utilised for measurements.

2.17.4. Total organic content. Samples were prepared for organic carbon analysis by following the HCl acidification method for the removal of carbonates according to Hedges and Stern (1984).[32] Subsequently, the acidified samples were analysed with an elemental analyzer (EA) (Vario PYRO Cube; Elementar Analysensysteme GmbH, Hanau, Germany). The EA was calibrated with sulphanilamide (N: 16.26%, C: 41.81%), the precision for carbon as a relative standard deviation was <5%.

2.18. Statistical analysis

Experimental data obtained were usually recorded in triplicate as a minimum and presented as mean values and the corresponding standard deviation (SD) and error bars when calculating standard error. *Post hoc* tests were carried out using the t-test with a one-tailed distribution. In all analyses, differences were accepted as significant when $p < 0.05$.

3. Results and discussion

3.1. Chemical structure

Vanillin cross-linked chitosan films containing gallic acid are denoted as CVGGA, where 'C', 'V', 'G' and 'GA' represent
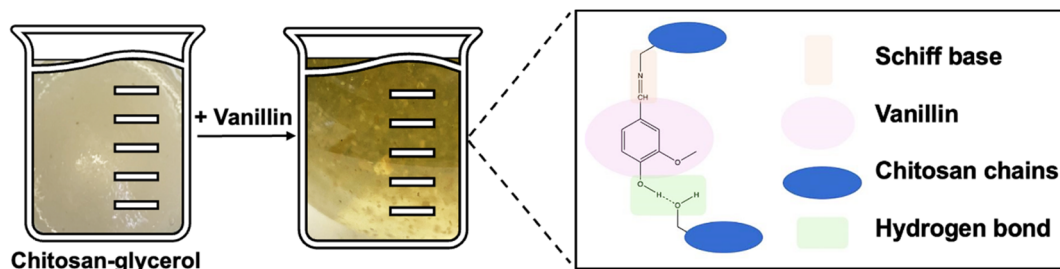
Fig. 1 Schematic of the synthesis of CVG cross linked films and the cross-linking mechanism.

chitosan, vanillin, glycerol and gallic acid, respectively. Therefore, CVG denotes the film without the added gallic acid, and CG denotes the non-cross-linked film. Fig. 1 shows a schematic of the mechanism of cross-linking between chitosan and vanillin, *via* the formation of a Schiff base and hydrogen bonding with chitosan chains. Gallic acid is added to this CVG solution in our study to form an active, degradable packaging material. We compare data of CVGGA films with our previous report on CVGP films, where 'P' represents Polyphenon 60 from green tea.[21]

Scanning electron microscopy (SEM) was used to investigate the surface morphology and microstructure of CVGGA films. The cross-linked films exhibited a smooth morphology with a compact structure (Fig. 2A). The SEM micrographs are indicative of the uniform mixing of film components.[33] The absence of voids suggests that there is a high degree of cross-linking in

the CVGGA films and may also be influenced by intermolecular hydrogen bonding between chitosan, vanillin and gallic acid.[12,33–36] This is consistent with our previous findings for CVGP films.[21]

UV radiation can cause photochemical damage and biological changes in food. Therefore, blocking UV light reduces food spoilage and enables the extension of food shelf-life, quality and safety. As a result of this, packaging materials often are designed with UV protection characteristics which may be induced with the use of fillers or additives.[37] Fig. 2B shows the UV blocking capacity of CG, CVG and CVGGA films. In accordance with previous literature, non-cross-linked chitosan films (CG) did not block UV light successfully.[38] However, both CVG and CVGGA films demonstrate 0% light transmission in the UV region (200–400 nm). From this, we can elucidate that the presence of the phenolic aldehyde vanillin and the Schiff base
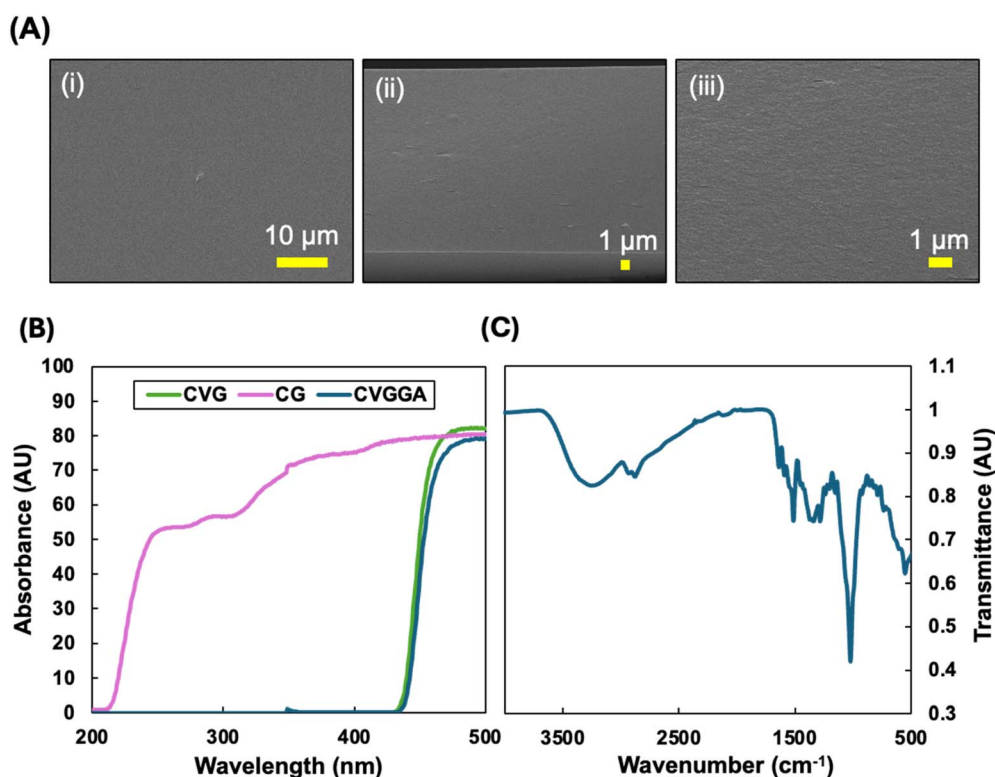

Fig. 2 (A) (i) Surface and (ii and iii) cross-sectional FE-SEM images of CVGGA films, (B) UV-blocking capacities of CG, CVG and CVGGA films, (C) FTIR spectrum of CVGGA.

interaction affords a material with the capacity to absorb UV light.[39] It is expected that the UV-blocking capacity is strengthened with the addition of gallic acid to the polymeric matrix due to UV-light absorbance *via* excitation of π-electrons in conjugated systems. Many literature studies report similar findings, with aromatic polyphenol extracts improving UV blocking properties.[36] Overall, the CVGGA films have strong UV barrier properties, which is a promising characteristic for food packaging materials.[37]

The cross-linking interaction between chitosan and vanillin was probed using FTIR analysis (Fig. 2C). FTIR spectroscopy has been utilised to confirm that natural phenolic aldehydes, including vanillin, conjugate with chitin through dynamic imine bonds.[40] Previously, we reported the shift in the vibration of a peak in the carbonyl region from 1656 to 1644 cm^{-1} between CG and CVG films.[21] This was consistent with the works of Zhang and Tomadoni and indicated the formation of a Schiff base.[11,12] An analysis of the full spectra revealed the broad peak at around 3275 cm^{-1}, indicative of OH stretching from hydroxyl groups and NH stretching from primary amine groups on glucosamine units. Peaks at 2932 cm^{-1} and 2875 cm^{-1} can be attributed to CH$_2$ and CH stretching respectively and the peak at 1635 cm^{-1} is due to carbonyl stretching. The peaks at 1511 cm^{-1} and 1347 cm^{-1} arise due to NH bending and CN stretching, respectively.[11] The intense peak around 1027 cm^{-1} is due to C–O stretching from β-(1,4) glycosidic bonds within the chitosan backbone. FTIR studies in recent literature have also confirmed interactions between phenolic extracts such as green tea with chitosan.[14,20,41] In this study, vanillin was added in the synthesis before gallic acid to ensure cross-linking was mostly between vanillin and chitosan, and that gallic acid acted as an additive which could be released.

3.2. Optical properties

The color of food packaging films is an important metric to consider, as consumers are more likely to accept colorless and transparent films. Chitosan films are usually yellow in color, but are visually transparent, allowing the consumer to assess the quality of the product. Table 1 shows the results from a colorimeter experiment of CVGGA films compared to CVG and CG films. Additionally, the yellowness index (YI) was calculated using eqn (1), and the opacity, recorded using UV-visible spectroscopy was calculated using eqn (2). The results presented in Table 1, when compared to our previous study and a study by Zhang *et al.* (2015), show that the CVGGA films are lighter, as

evidenced by a higher value of L^*.[12] Correlating with literature, the non-cross-linked film (CG) has a lower b^* value than vanillin-containing films, indicating that the cross-linking interaction increases the yellowness of the films.[11,12] This observation is evidenced in the increase of the yellowness index between CG and CVG. CVGGA has the highest value for the yellowness index, this could suggest some cross-linking with the addition of gallic acid. The opacity values increase with cross-linking interactions, and CVG data correlates well with the values reported by Zhang *et al.* (2015) for similar films with a value of 1.128 ± 0.015.[12]

Whilst darker films can preserve light-sensitive foods, it is likely that they will be met with consumer non-acceptance. To this end, we measured the colour change of CVGGA and CVG films over 12 weeks of aging in an ambient environment. We observed small changes in the L^*, a^* and b^* values, with associated changes in the yellowness index values. Importantly, there was no significant difference in the opacity of aged CVGGA films when compared to fresh CVGGA films. This result presents an advantage over our previous research in which Polyphenon 60 was utilised as the active compound, and films browned significantly over time due to polyphenol oxidation.[21]

3.3. Water-sensitivity

Bare chitosan films have high water-sensitivity and form hydrogels in aqueous environments. However, the strong network of cross-linking in chitosan–vanillin composites affords films with reduced sensitivity to water and prevents hydrogel formation. Table 2 shows the moisture content, water contact angle and water solubility data for CVGGA, CVG and CG films. The results show that the moisture content decreases with vanillin cross linking, as expected, and decreases further with the addition of gallic acid. This can be explained by a reduction in the number of free amine and hydroxyl groups in

Table 2 Moisture content, water contact angle and water solubility data for chitosan films[a]

Film	MC	WCA (θ)	WS
CVGGA	11.5 ± 0.1^a	44.5 ± 0.7^a	19.9 ± 1.2^a
CVG	14.9 ± 0.3^b	36.5 ± 3.5^b	18.0 ± 0.8^a
CG	27.5 ± 0.8^c	81.4 ± 2.5^c	38.4 ± 0.8^c

[a] a, b, c different letters within the same column indicate significant differences over time ($p < 0.05$).

Table 1 Color and opacity values for CG, CVG and CVGGA films[a]

Film	YI	L^*	a^*	b^*	Opacity
CVGGA	55.7	88.2 ± 0.3^a	-4.2 ± 0.2^a	34.4 ± 1.5^a	2.1 ± 0.4^a
CVGGA (aged)	60.7	85.0 ± 0.5^b	1.3 ± 0.4^b	36.1 ± 0.8^a	2.3 ± 0.5^a
CVG	42.9	84.3 ± 0.5^b	0.8 ± 0.2^b	25.3 ± 0.5^b	1.3 ± 0^b
CVG (aged)	38.5	89.1 ± 0.3^c	-1.5 ± 0.2^c	24.0 ± 0.5^c	1.44 ± 0^c
CG	8.8	88.8 ± 0.7^a	-0.2 ± 0^d	5.5 ± 0.4^d	1.2 ± 0.1^b

[a] a, b, c, d different letters within the same column indicate significant differences over time ($p < 0.05$).

the chitosan matrix, as they are utilised in cross-linking interactions. Moreover, this suggests that there are stronger intermolecular interactions in the CVGGA film, which may be attributed to hydrogen bonding. Literature studies have also suggested that glycerol interacts with gallic acid within chitosan matrix, further reducing the moisture content.[39] Overall, these results correlate well within the literature, where Zhu *et al.* (2022) reported a moisture content of 11.79% for their chitosan–ethyl vanillin film and Bhowmik *et al.* (2024), who reported a moisture content of 17.01% for their chitosan–glycerol–chitooligosaccharides–gallic acid films.[39,42]

The results detailed in Table 2 also show that CVGGA and CVG films are hydrophilic, with water contact angles below 90° and as widely reported in the literature, the bare chitosan film surface was less hydrophilic.[21] The increase in the water contact angle between CVG and CVGGA suggests further interactions of free amines or hydroxyl groups on the surface of the chitosan film, making them unavailable for interactions with water. Water contact angle images can be found in the ESI (Fig. S5).† This indicates that gallic acid interacts with these groups *via* cross-linking or hydrogen bonding. Furthermore, the bare chitosan film exhibited the highest solubility in water at 38.4 ± 0.8%, with CVG and CVGGA films having lower solubility values. As previously described for the moisture content and water contact angle values, this reduction in water-solubility can be attributed to stronger interactions within the CVG and CVGGA polymer matrices, with fewer functional groups available for hydrogen bonding with water. A reduced water solubility can offer improved tensile properties by reducing plasticization effects.[43] Furthermore, the reduced water solubility of CVGGA films indicates an improved moisture barrier of the packaging material and relates to successful application in its eventual use as food packaging in high moisture environments such as fridges.

3.4. Permeability

Good barrier properties are essential for food packaging applications. Successful food packaging should protect food from moisture and degradation-enhancing gases. The water vapour permeability of films depends on the film thickness, the film structure and functional groups, and the experimental conditions. The SEM micrographs of CVGGA films (Fig. 2A) showed a compact structure without pores or channels, suggesting a promising material for good barrier properties. Table 3 shows the water vapour permeability data for both CVGGA and CVG films.

We determined that CVGGA films had a lower WVP value than CVG films. This correlates well with the water-sensitivity

data, which suggested that there are stronger interactions within this polymer matrix, and fewer available hydroxyl and amine groups. This is consistent with literature reports, and the values of WVP achieved here are generally lower than similar research studies, indicating improved permeability.[12,39,42] The values of WVP are similar to a recent report by Bhat *et al.* (2022) on a chitosan–guar gum–poly(vinyl alcohol)–moringa extract active material, which was reported to have a WVP of $5.37 \pm 1.70 \times 10^{-10}$ g m^{-1} s^{-1} Pa^{-1}.[44] WVTR values were determined using the linear regression data from laboratory experiments of mass-loss over time (Fig. S1, ESI†).

3.4. Thermal properties

Thermal properties are important for biopolymers as they relate to their stability and future processability in scale-up operations. DSC analysis shows how polymers react to heat and provide important metrics relating to a material's thermal use limits including the glass transition temperature (T_g). Fig. 3A shows the DSC trace with two endothermic peaks at (i) 128.9 °C and (ii) 274.0 °C, relating to the loss of bound water (i) and the glass transition temperature (ii). TGA analysis investigates the thermal stability of polymers and the resulting trace of mass loss against temperature is shown in Fig. 3B. The initial mass loss of 11.8% up to 130 °C relates to the loss of bound water from the polymer matrix.[11,21] This value is often used to elucidate the moisture content in polymer films and is very similar to the experimental value we determined in Table 2. The first degradation stage between 130 °C and 220 °C amounted to a mass loss of 20.2%. The second degradation stage between 220 °C and 305 °C amounted to a mass loss of 23% and can be attributed to the onset of chitosan polymer degradation. Between 305 °C and 600 °C, there was a further mass loss step of 12%, with 33% mass remaining as char at the end of the experiment. This char would be expected to decompose at temperatures above 600 °C. The temperature at which there was the maximum rate of mass loss (T_{max}) was determined as 189 °C. This is similar to the result we determined for CVGP films as 220 °C, in this study we also confirmed that cross-linking with vanillin increases the decomposition temperature of chitosan films.[11,12,21]

3.5. Mechanical properties

The mechanical properties of biopolymer films determine their resistance to damage during consumer handling, storage and transportation. The tensile strength and flexibility (elongation at break) are important metrics relating to food packaging materials and indicate the potential success of the material in

Table 3 Water vapor permeability values for CVGGA and CVG films[a]

Film	Thickness (μm)	WVP (g m^{-1} s^{-1} Pa^{-1})	WVTR (g m^{-2} s^{-1})
CVGGA	68.5 ± 2.7[a]	$1.99 \times 10^{-10} \pm 2.1 \times 10^{-11,a}$	0.006 ± 0.002[a]
CVG	64 ± 3.5[a]	$2.46 \times 10^{-10} \pm 1.2 \times 10^{-11,b}$	0.008 ± 0.002[b]

[a] a, b different letters within the same column indicate significant differences over time ($p < 0.05$).
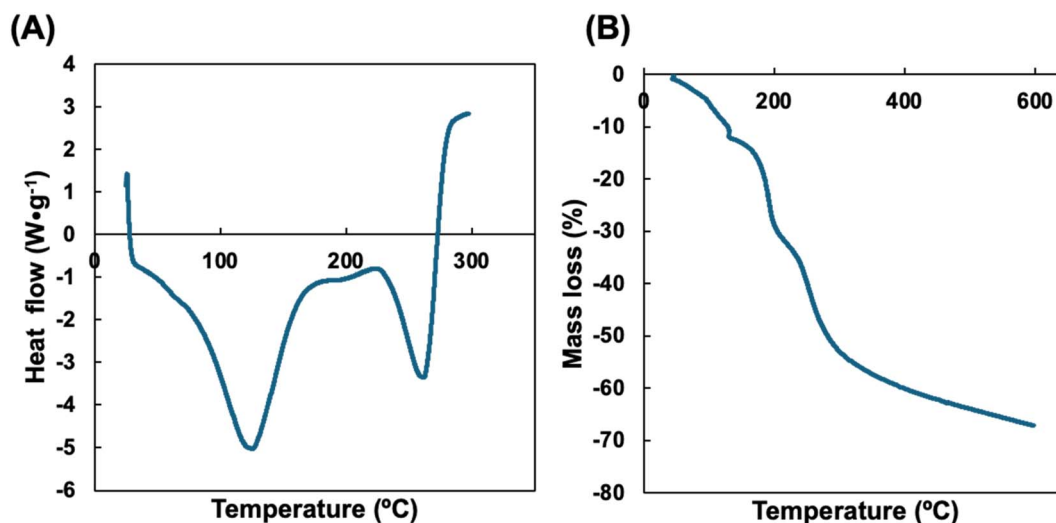
Fig. 3   (A) DSC and (B) TGA data for CVGGA films.

being able to wrap around food without cracking or ripping. Table 4 shows the mechanical properties of CVGGA films and compares fresh films to those which have been stored in an ambient environment for 12 weeks to determine the effect of aging and long-term stability. The force at break was determined as 29.4 ± 0.5 for fresh CVGGA films and was found to decrease to 18.8 ± 1.2 over time. The elongation at break or displacement, was found to increase over time from $5.4 \pm 1\%$ to $7.3 \pm 1.5\%$ and Young's modulus (YM) decreased from 1232 ± 30 MPa to 756 ± 43 MPa. An image of the tensile strength experiments can be found in the ESI (Fig. S6).† The reduction in YM and force at break values, coupled with the increase in displacement, indicates a slight deterioration in properties over time. We observed minimal changes in color in the aging experiment for CVGGA films, however it is possible that some gallic acid is oxidized to quinones over time. This may explain the reduction in tensile strength as the aromatic phenol groups would then be unavailable for interactions via hydrogen bonding or cross-linking.

The results presented in Table 4 are similar to those determined during our previous work on CVGP films, with improved force at break values indicating superior intermolecular forces in the CVGGA films.[21] The values correlate well with similar literature studies by Tomadoni et al. (2019) who reported a YM value for their optimized CVG film, dried at 57.5 °C as 1225 ± 135 MPa, this is similar to the value we report for our CVGGA film.[11] Zhang et al. (2015) also reported maximum values of

10.18 ± 0.41 N (force at break) and $43.73 \pm 2.03\%$ (elongation at break) for their chitosan–vanillin film.[12] The group's value for elongation at break is significantly larger than what we report, suggesting that this metric could be optimised in our material by altering the cross-linker or plasticiser content. Overall, the films have promising mechanical properties with good tensile strength and flexibility.

3.6. Controlled release behaviour

The controlled release of the active compound enables active packaging to elicit antioxidant and antimicrobial effects successfully over a longer period. Cross-linking techniques are often utilised to prevent polymer swelling and enable the controlled release of a compound from within a polymer matrix by reducing diffusion pathway lengths.[21] The release of compounds from biopolymer composites is usually governed by random molecular diffusion in the direction of the concentration gradient and may involve an initial 'burst release' involving surface-adsorbed or near-surface molecules, followed by controlled release from within the bulk of the polymer.[45,46] The rate of release depends on many factors including polymer degradation, polymer swelling, the food simulant used, the polarity of the active compound, the strength of binding interactions between the polymer and the active compound, polymer molecular weight, film thickness, temperature and pH values. The substrate used for testing is not standard in the literature and varies between food simulants, which are more commonly

Table 4   Mechanical properties of CVGGA films[a]

Film	Force at break (N)	Tensile strain (%)	Tensile stress (MPa)	Displacement (mm)	Young's modulus (MPa)
CVGGA	29.4 ± 0.5^a	4.4 ± 0.8^a	25.0 ± 2.8^a	5.4 ± 1.0^a	1232 ± 30^a
CVGGA (aged)	18.8 ± 1.2^b	7.1 ± 1.0^b	19.4 ± 1.4^b	7.3 ± 1.5^b	756 ± 43^b

[a] a, b different letters within the same column indicate significant differences over time ($p < 0.05$).

used, and actual food. Food simulants include 95% ethanol (v/v) for high fat content foods, pure water for aqueous media, 50% ethanol (v/v) for oil in water emulsions or high alcohol content foods and 3% acetic acid (v/v) for low pH aqueous foods.[47] Lopez-Cordoba *et al.* (2017) described the change in the release profile of polyphenols in different food simulants.[48] For our study, a lipophilic food simulant was chosen due to the compatibility with our chitosan film and gallic acid solubility characteristics.

Fig. 4A shows the release profile of gallic acid into the food simulant over 2 weeks. We studied the release cumulatively over this extended timeframe to relate this release to the rate of food degradation. We observed an initial burst release within the first 24 hours of the study, in which 40% of the total mass of

gallic acid was released. The total amount released after 2 weeks amounted to 82.9% of the gallic acid content calculated for the film sample based on homogeneity assumptions. Fig. 4B shows SEM images of the cross-section of CVGGA films during the release study. The SEM micrographs show a less closely packed structure in comparison to the bare CVGGA films (Fig. 2A), and this suggests the formation of diffusion channels for gallic acid release. Initially, the release profile was fit to zero-and first order kinetics with R^2 values of 0.83 and 0.53, respectively (Fig. S7, ESI†). The release profile was then fit to the Korsmeyer–Peppas and Higuchi kinetic models (Fig. 4C and D). The Korsmeyer–Peppas model describes release from a hydrophilic erodible polymer and the release exponent 'n' (eqn (10)) is used to indicate the release mechanism. Fickian transport is evaluated
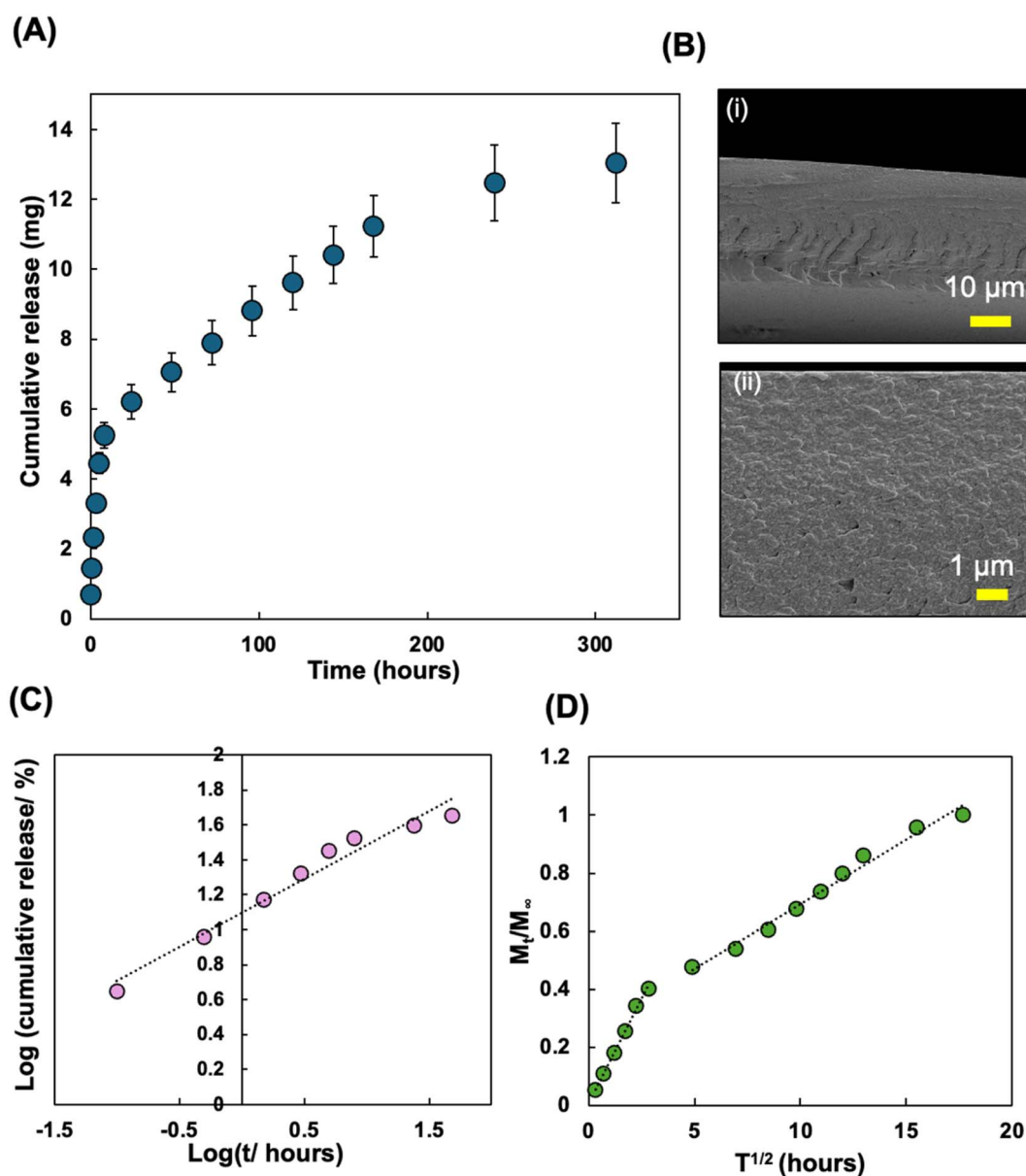

Fig. 4 (A) Controlled release of gallic acid from CVGGA films, (B) cross-sectional FE-SEM images of CVGGA films during release study, (C) Korsmeyer–Peppas model and (D) Higuchi model of the release data.

when the release exponent value is 0.45. For our CVGGA films, n was calculated as 0.39, suggesting hindered Fickian transport, in which the release is governed by diffusion and other mechanisms. The Higuchi model describes release from a solid matrix (eqn (11)). For our release data, we treated the initial release and controlled release as two 'phases' for this model. The kinetic constants for release were calculated using eqn (10)–(12). K_{KP} was determined as 12.4 h^{-n} with a R^2 value of 0.97, K_H for the initial release was determined as 0.14 h^{-1} with a R^2 value of 0.99, and K_H for the controlled release was determined as 0.045 h^{-1} with a R^2 value of 0.99. We also determined the diffusion coefficient (D) for the initial burst release using eqn (12) and (13), calculating a value of 1.39×10^{-7} m^2 s^{-1}.

The calculated diffusion coefficient is higher than the value we reported for CVGP films in a simulant of 50% (v/v) ethanol–water, suggesting that the lipophilic food simulant and gallic acid as the active compound is more effective at release.[21] However, López de Dicastillo *et al.* reported an increase in the release of gallic acid in aqueous food simulants in comparison to lipophilic simulants.[49] The group also reported that kinetically, gallic acid showed faster diffusivity than other components of green tea extract due to its small molecular size and solubility characteristics.[49] In our previous study, we evaluated that there was no significant loss in release characteristics after 1 month of storage in a controlled environment.[21] Importantly, when applied to food, we expect that direct contact will induce gallic acid release. Another significant consideration for the eventual use as a food contact material is the migration limits of packaging components. Vitally, gallic acid is approved for use as an additive in polymer materials and vanillin is approved as a flavouring agent in food.

3.7. Antioxidant and antimicrobial properties

Strong antioxidant and antimicrobial properties are vital for extending the shelf life of food, protecting it from unwanted changes during storage, processing and transportation, specifically oxidation and microbial attack. Gallic acid is a strong natural antioxidant due to its phenol moiety acting as a radical scavenger. We carried out a DPPH assay on CVGGA films, CVG films and gallic acid to determine the antioxidant properties of these materials. Fig. 5A shows the results of the DPPH assay, in which both CVGGA films and gallic acid at a concentration of 10 mg mL^{-1} reduced >98% of DPPH radicals, indicating excellent antioxidant capacities. The CVG film reduced 79% of the DPPH radicals, confirming that this material has good antioxidant capacity, but gallic acid provides improved, synergistic, antioxidant capabilities to the film. The concentration of gallic acid used in this assay can be related to the release study, in which the maximum concentration was 36 mg mL^{-1}. The results are consistent with Li *et al.* who reported a DPPH inhibition of 82.2% for their chitosan–vanillin derived dialdehyde material.[50] Similarly, Yu *et al.* reported that vanillin improved the antioxidant activity of their chitosan–gelatine film.[33] We postulate that gallic acid has a synergistic effect, further increasing the antioxidant scavenging capacity of the film. This is consistent with the work of Bhowmik *et al.*, who determined
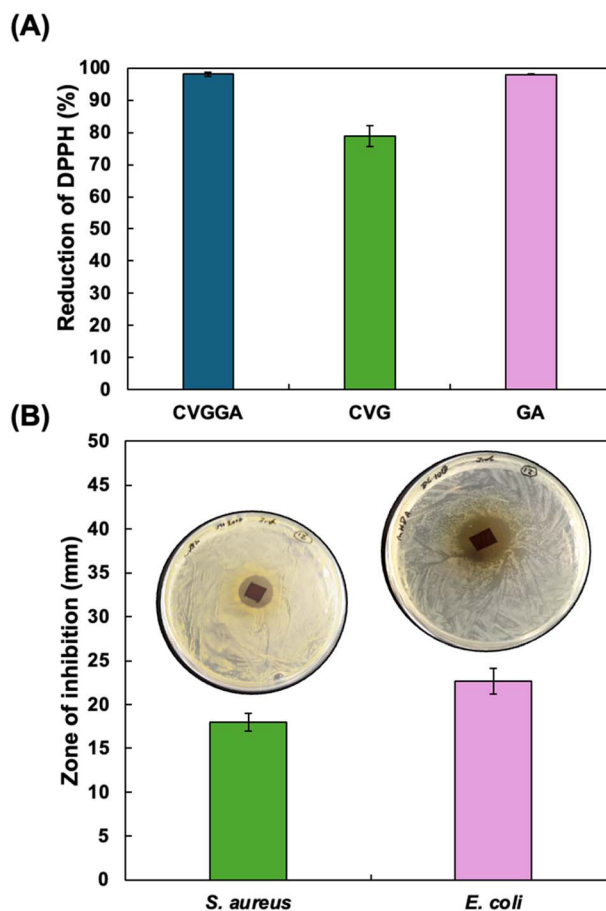

Fig. 5 (A) DPPH antioxidant activity of CVGGA films, CVG films and gallic acid at 10 mg mL^{-1}, (B) antimicrobial efficacy of CVGGA films against *S. aureus* and *E. coli*.

that gallic acid increased the antioxidant activity of their chitosan films.[39] The results we report are similar to those reported by Peng *et al.* who determined a percentage reduction of 94.9% for their chitosan films incorporated with tea extracts.[41]

Pieces of CVGGA film were then tested for their antibacterial activity against *S. aureus* and *E. coli* by zone of inhibition (ZOI) tests (Fig. 5B). The ZOI values showed successful inhibition of both bacterial strains with these small pieces of CVGGA film. ZOI values for viscous film-forming solutions of CG, CVG and CVGGA against *S. aureus* and *E. coli* were also evaluated as 8.7 ± 0.3 mm, 8 ± 0.6 mm, 4.7 ± 2.4 mm and 9 ± 1 mm, 10.3 ± 1.2 mm, 5.7 ± 2.8 mm, respectively (Fig. S8, ESI†). Further to this, the minimum inhibitory concentration (MIC) values for vanillin and gallic acid against *E. coli* were determined as 2.5 mg mL^{-1} and 5 mg mL^{-1} respectively, with MIC values of 5 mg mL^{-1} and 10 mg mL^{-1} for *S. aureus* (Fig. S9, ESI†). Li *et al.* recently reported a significant increase in antibacterial activity between chitosan films and films incorporating a vanillin derived dialdehyde.[50] The group determined that bare chitosan exhibited a weak inhibitory effect which may be explained by the disruption of bacterial cell walls through electrostatic binding *via* protonated functional groups on chitosan film surfaces.[50]

Overall, the antibacterial data confirms the ability of this CVGGA film to prevent the growth of both *E. coli* and *S. aureus*.

3.8. Degradation

The degradability of natural polymers is important to determine for innovation and circularity metrics. Degradation usually occurs by biodeterioration, fragmentation, assimilation and then mineralisation and metabolism. Degradable natural polymer materials are eventually degraded to CO_2, CH_4, water, biomass and humic matter. The degradation rate of biopolymers depends on the polymer chain length, complexity, crystallinity, molecular weight and strength of interactions within the matrix.[51] Other factors include the degradation environment, light intensity, temperature, moisture content, oxygen availability and pH value. In soil, microorganisms including bacteria, fungi and enzymes act to increase the degradation rate. Hydrolysis by water is also a possible mechanism of degradation, and it is likely that a higher moisture content environment allows for bulk degradation *via* the diffusion of water into the polymer matrix.

We studied the degradation of CVGGA films in soil, seawater and water over a period of 12 weeks (Fig. 6A). We also tested samples which we submerged in lipophilic food simulant for 24

hours and rinsed with water before burying in soil, termed as lifecycle soil degradation. This experiment probed the effect of reducing the concentration of active antimicrobial compounds (gallic acid, vanillin) from within the film *via* release studies. We hypothesised that this may increase microbial activity and therefore, degradation. Indeed, Kaczmarek-Szczepánska *et al.* noted that antimicrobial properties of films make biodegradation more difficult, requiring the activity of resistant microorganisms.[52] For all experiments in soil, we added water at regular intervals to simulate natural precipitation, and seawater samples were topped up in the case of evaporation. The moisture content of soil was determined by mass balance as 43.4%, indicating a good availability of water molecules to aid the degradation of CVGGA. Water increases degradation by interrupting intermolecular forces and the permeation of water into the matrix relates to the onset of bulk degradation.[53] Furthermore, we measured the pH of soil as 5.66, indicating a mildly acidic environment. It is possible that imine groups would be protonated in this environment, making them more susceptible to hydrolysis.[54]

We found that, after 12 weeks, CVGGA samples in soil and lifecycle soil both exceeded 90% mass loss, satisfying current criteria for compostable materials. The mass loss for samples in seawater and water was determined as $43.1 \pm 6.7\%$ and $32.6 \pm 0.9\%$, respectively. These results are consistent with our previous findings, concluding that degradation in seawater occurs at a reduced rate and consists mostly of fragmentation.[21] Distinctly from this study, for CVGP films, we found improved degradation in compost when compared to soil samples.[21] The likely explanation for this is a different batch of soil containing different bacterial quantities and strains in each case. Importantly, in all cases, biodegradation is evidenced by mass loss of the cross-linked chitosan films. During degradation, we also investigated the changes in morphology of CVGGA films using FE-SEM, and SEM micrographs of films at 3, 6 and 9 weeks of degradation in soil can be found in the ESI (Fig. S10).†

We carried out FTIR analysis to begin to probe the degradation mechanism for CVGGA films. Fig. 6C shows the FTIR spectra of degraded CVGGA films compared to fresh CVGGA films, focusing on the peak at 1024 cm^{-1}, corresponding to C–O stretching and bending. The degraded sample has a less intense peak in this region when compared to other peaks present in both spectra which have similar relative intensities, indicating that there are fewer of these bonds present after degradation. This can be observed more clearly when comparing the relative intensities of the peaks at 1024 cm^{-1} and 1063 cm^{-1}. We can elucidate that this observation is due to the cleavage of glycosidic (C–O–C) bonds within the chitosan backbone, likely by enzymatic action. Enzymes such as chitinase, chitosan deacetylase, β-*N*-acetylglucosaminidase and lysozyme are present in soil samples, and this is a likely mechanism of degradation to form smaller chitosan oligosaccharides in the first instance. Overall, the decrease in C–O bonds can indicate the decomposition of chitosan into smaller units. Furthermore, the DDA% of chitosan is important and relates to the degradation capacity. Commercial chitosan has a DDA% of >75%. Higher DDA%
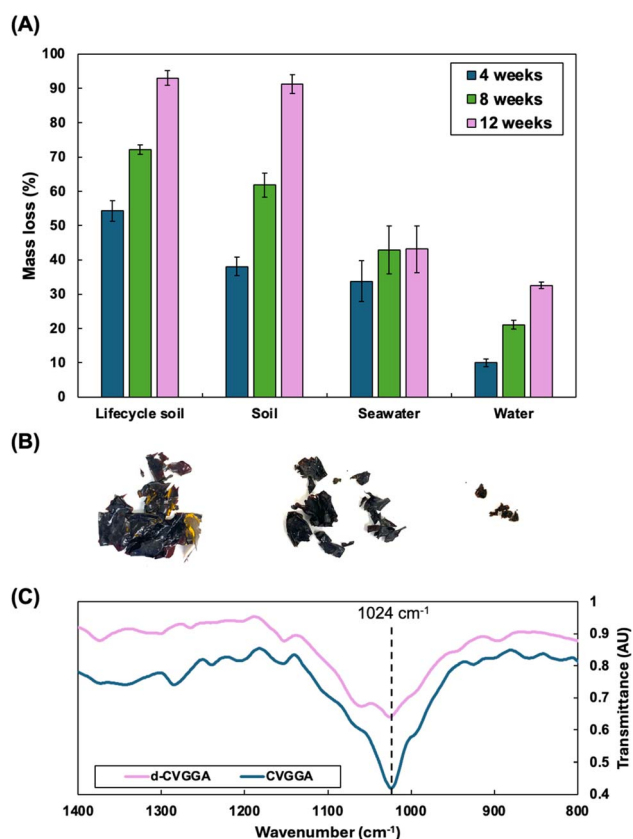

Fig. 6 (A) Degradation of CVGGA films in soil after submersion in food simulant (lifecycle), soil, seawater and water, (B) images of CVGGA films during degradation in soil, taken after rinsing with water and drying, (C) FTIR comparison of CVGGA and soil-degraded CVGGA films.

Table 5 Glass transition temperature of CVGGA and TOC of soil over time during degradation

Value	0 weeks	6 weeks	12 weeks
T_g CVGGA (DSC)/°C	274.0	262.4	214.8
TOC (soil)/%	18.2 ± 0.5	22.3 ± 0.1	25.1 ± 0.8

values indicate improved degradation rates as chitosan deacetylase activity is not required to break down these fragments.

Table 5 shows further investigation into the degradation of CVGGA films in soil over time. We investigated the reduction in the glass transition temperature during degradation, and the increase in the total organic content of soil, probing the degradation of the biopolymer film. The reduction in the T_g value indicates a reduction in the molar mass of the chitosan in the film, indicating depolymerisation by the cleavage of β-1,4-glycosidic bonds in the backbone of the polymer.[54] In addition to this degradation data, we further probed our mechanistic interrogations with repeated degradation studies (Fig. 7) and a DSC-UV investigation, which concluded that there were no changes to the heat flow of the polymer film during UV treatment (Fig. S11, ESI†).

We carried out further degradation tests on CVGGA, CVG and CG films including a 24 week degradation study in soil with no disturbance (Fig. 7). We found that all 3 films degraded completely under these conditions. We also carried out degradation tests of CVGGA films in autoclaved soil, a home compost bin, and outside. The investigation utilising autoclaved soil was carried out to probe if there was any degradation without microbial activity. We determined that the films degraded to $34.1 \pm 1.6\%$ under these conditions and conclude that this fragmentation was due to water hydrolysis and swelling. To probe the effect of the fluctuating conditions of field tests, rather than controlled laboratory conditions, we buried film samples in a large compost bin and measured the mass loss after 24 weeks. This experiment reached a mass loss of $63.6 \pm 1.6\%$, however we utilised nylon mesh bags to hold the samples

in for ease of retrieval, therefore it is likely that this value would increase with complete integration into the compost mixture. Finally, the degradation in the open-air environment was determined as $35 \pm 7.9\%$. The DSC-UV results, presented in the ESI (Fig. S11),† suggest that there was no photodegradation after UV irradiation for 2 h. Therefore, it is likely that this mass loss may be due to hydrolysis *via* precipitation.

Further to this, TGA-MS (EGA) was carried out to investigate thermal degradation products and relate this to the potential mechanism for CVGGA degradation in soil. TGA-MS (EGA) data showed relevant m/z peaks at (i) 211 °C, (ii) 326.5 °C, (iii) 406.5 °C and (iv) 602.3 °C (Fig. S12, ESI†). The first timepoint of interest (i) includes a peak at m/z 17, indicating the formation of NH_3 as a volatile product. The second timepoint (ii) has a peak at m/z 125 which may indicate the formation of 3-acetamido furan *via* dehydration and ring-opening mechanisms.[55] The third timepoint (iii) has a peak at m/z 67, which may indicate the formation of pyrrole *via* thermal degradation.[55,56] Indeed, Liu *et al.* proposed potential mechanisms for the formation of pyrrole compounds and 3-acetamidofuran from the pyrolysis of chitosan and chitin, respectively.[55] Finally, the fourth timepoint (iv) has a peak at m/z 179, which may indicate the formation of glucosamine *via* cleavage of the glycosidic bond in the chitosan backbone. A schematic depiction of the potential mechanism for CVGGA degradation in soil, after consideration of all analytical techniques and the resulting data, can be seen in Fig. 8.

Overall, the degradation results revealed that CVGGA films are degradable to >90% in soil within 12 weeks and 100% within 24 weeks. We found that releasing some of the active components by submersion in food simulants before degradation enhanced this capacity, likely due to a reduction in microbial inhibition and therefore an increase in microbial activity. We observed only fragmentation in seawater and water environments, elucidating that these are not appropriate end-of-life environments for this material. FTIR data confirmed the reduction in C–O bonds during degradation, relating to the hydrolytic cleavage of the chitosan backbone, producing oligomers of chitosan. This is consistent with our observation that the glass transition temperature of polymer samples reduced during degradation, relating to a reduction in polymer molecular weight and chain length. This is coupled with the increase in the organic content of soil samples during degradation, indicating the assimilation of degradation product such as organic acids. Similarly, TGA-MS-EGA analysis revealed the potential formation of glucosamine units. We also elucidated the effect of soil bacteria on degradation with a comparison to the use of autoclaved soil, concluding that microorganisms are vital to achieve high levels of decomposition. Future work should probe the enzymes present in the soil samples and determine the mechanism of degradation in scalable environments. Beyond the degradation of the material, we also investigated physiochemical properties and found that CVGGA has good barrier properties, tensile strength and UV-blocking properties. Furthermore, we confirmed the strong antioxidant and antimicrobial capacities of CVGGA films utilising a DPPH assay, and *E. coli* and *S. aureus* inhibition. Conclusive of this,
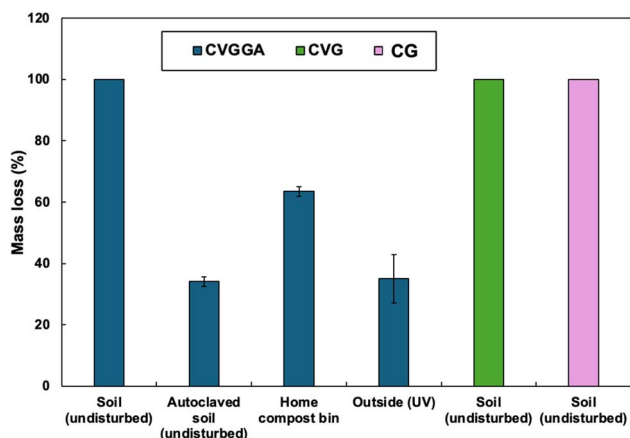
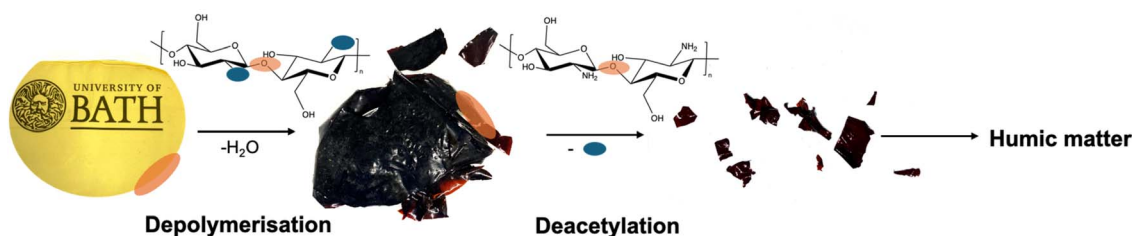**Fig. 7** Degradation capacities of CVGGA, CVG and CG films in different environments at 24 weeks.

Fig. 8 Schematic of the proposed mechanism of degradation for CVGGA films, where the first stage involves depolymerisation *via* hydrolytic cleavage of glycosidic bonds, likely starting at the outside of the film, followed by deacetylation and cleavage of Schiff-base bonds, followed by further degradation and assimilation to humic matter.

the presented CVGGA material is a strong candidate for future development of sustainable active packaging materials.

Data availability

The data supporting this article have been included as part of the ESI.† More detailed data will be available upon request from the authors.

Conflicts of interest

There are no conflicts to decare.

Acknowledgements

References

1 S. Shaikh, M. Yaqoob and P. Aggarwal, An overview of biodegradable packaging in food industry, *Curr. Res. Food Sci.*, 2021, **4**, 503–520, DOI: **10.1016/j.crfs.2021.07.005**.

2 J. Rocha-Pimienta, B. Navajas-Preciado, C. Barraso-Gil, S. Martillanes and J. Delgado-Adámez, Optimization of the Extraction of Chitosan and Fish Gelatin from Fishery Waste and Their Antimicrobial Potential as Active Biopolymers, *Gels*, 2023, **9**(3), 254.

3 M. Iñiguez-Moreno, B. Santiesteban-Romero, E. M. Melchor-Martínez, R. Parra-Saldívar and R. B. González-González, Valorization of fishery industry waste: chitosan extraction and its application in the industry, *MethodsX*, 2024, **13**, 102892, DOI: **10.1016/j.mex.2024.102892**.

4 J. L. Vidal, T. Jin, E. Lam, F. Kerton and A. Moores, Blue is the new green: valorization of crustacean waste, *Curr. Res. Green Sustainable Chem.*, 2022, **5**, 100330, DOI: **10.1016/j.crgsc.2022.100330**.

5 R. Priyadarshi and J.-W. Rhim, Chitosan-based biodegradable functional films for food packaging applications, *Innovative Food Sci. Emerging Technol.*, 2020, **62**, 102346, DOI: **10.1016/j.ifset.2020.102346**.

6 F. L. Muñoz, S. Meramo, L. Ricardez-Sandoval, A. D. Gonzalez, B. C. Castillo, A. G. Quiroga, B. L. G. Baptiste and J. León-Pulido, Insights from an exergy analysis of a green chemistry chitosan biorefinery, *Chem. Eng. Res. Des.*, 2023, **194**, 666–677, DOI: **10.1016/j.cherd.2023.04.038**.

7 S. Suresh, M. Umesh and A. S. Santosh, Biological extraction of chitin from fish scale waste using proteolytic bacteria Stenotrophomonas koreensis and its possible application as an active packaging material, *Biomass Convers. Biorefin.*, 2024, **14**(22), 29023–29033, DOI: **10.1007/s13399-023-03865-y**.

8 C. P. Jiménez-Gómez and J. A. Cecilia, Chitosan: A Natural Biopolymer with a Wide and Varied Range of Applications, *Molecules*, 2020, **25**(17), 3981, DOI: **10.3390/molecules25173981**.

9 L. Zhuang, X. Zhi, B. Du and S. Yuan, Preparation of Elastic and Antibacterial Chitosan–Citric Membranes with High Oxygen Barrier Ability by in Situ Cross-Linking, *ACS Omega*, 2020, **5**(2), 1086–1097, DOI: **10.1021/acsomega.9b03206**.

10 H. J. Wiggers, P. Chevallier, F. Copes, F. H. Simch, F. D. Veloso, G. M. Genevro and D. Mantovani, Quercetin-Crosslinked Chitosan Films for Controlled Release of Antimicrobial Drugs, *Front. Bioeng. Biotechnol.*, 2022, **10**, 814162, DOI: **10.3389/fbioe.2022.814162**.

11 B. Tomadoni, A. Ponce, M. Pereda and M. R. Ansorena, Vanillin as a natural cross-linking agent in chitosan-based films: optimizing formulation by response surface methodology, *Polym. Test.*, 2019, **78**, 105935, DOI: **10.1016/j.polymertesting.2019.105935**.

12 Z. H. Zhang, Z. Han, X. A. Zeng, X. Y. Xiong and Y. J. Liu, Enhancing mechanical properties of chitosan films via modification with vanillin, *Int. J. Biol. Macromol.*, 2015, **81**, 638–643, DOI: **10.1016/j.ijbiomac.2015.08.042**.

13 D. Carrizo, G. Gullo, O. Bosetti and C. Nerín, Development of an active food packaging system with antioxidant properties based on green tea extract, *Food Addit. Contam.,: Part A*, 2014, **31**(3), 364–373, DOI: **10.1080/19440049.2013.869361**.

14 U. Siripatrawan and B. R. Harte, Physical properties and antioxidant activity of an active film from chitosan incorporated with green tea extract, *Food Hydrocolloids*, 2010, **24**(8), 770–775, DOI: **10.1016/j.foodhyd.2010.04.003**.

15 X. Liu, F. Xu, H. Yong, D. Chen, C. Tang, J. Kan and J. Liu, Recent advances in chitosan-based active and intelligent packaging films incorporated with flavonoids, *Food Chem.: X*, 2025, **25**, 102200, DOI: **10.1016/j.fochx.2025.102200**.

16 P. Shan, K. Wang, F. Yu, L. Yi, L. Sun and H. Li, Gelatin/sodium alginate multilayer composite film crosslinked with green tea extract for active food packaging application, *Colloids Surf., A*, 2023, **662**, 131013, DOI: **10.1016/j.colsurfa.2023.131013**.

17 D. Hamann, B. M. S. Puton, T. Comin, R. Colet, E. Valduga, J. Zeni, J. Steffens, A. Junges, G. T. Backes and R. L. Cansian, Active edible films based on green tea extract and gelatin for coating of fresh sausage, *Meat Sci.*, 2022, **194**, 108966, DOI: **10.1016/j.meatsci.2022.108966**.

18 I. Rahmawati, A. W. Pratama, S. A. Pratama, M. N. Khozin, A. Firmanda, F. H. Irawan, Asranudin, A. N. M. Ansori and T. H. Sucipto, Gallic acid: a promising bioactive agent for food preservation and sustainable packaging development, *Case Stud. Chem. Environ. Eng.*, 2024, **10**, 100776, DOI: **10.1016/j.cscee.2024.100776**.

19 H. Wang, J. Qian and F. Ding, Emerging Chitosan-Based Films for Food Packaging Applications, *J. Agric. Food Chem.*, 2018, **66**(2), 395–413, DOI: **10.1021/acs.jafc.7b04528**.

20 C. De Carli, V. Aylanc, K. M. Mouffok, A. Santamaria-Echart, F. Barreiro, A. Tomás, C. Pereira, P. Rodrigues, M. Vilas-Boas and S. I. Falcão, Production of chitosan-based biodegradable active films using bio-waste enriched with polyphenol propolis extract envisaging food packaging applications, *Int. J. Biol. Macromol.*, 2022, **213**, 486–497, DOI: **10.1016/j.ijbiomac.2022.05.155**.

21 J. R. Westlake, M. Laabei, Y. Jiang, W. C. Yew, D. L. Smith, A. D. Burrows and M. Xie, Vanillin Cross-Linked Chitosan Film with Controlled Release of Green Tea Polyphenols for Active Food Packaging, *ACS Food Sci. Technol.*, 2023, **3**(10), 1680–1693, DOI: **10.1021/acsfoodscitech.3c00222**.

22 ASTM, D., *The American Society for Testing and Materials, D 6442-99*, 2000.

23 S. Y. Park, K. S. Marsh and J. W. Rhim, Characteristics of Different Molecular Weight Chitosan Films Affected by the Type of Organic Solvents, *J. Food Sci.*, 2002, **67**(1), 194–197, DOI: **10.1111/j.1365-2621.2002.tb11382.x**.

24 K. N. Turhan and F. Şahbaz, Water vapor permeability, tensile properties and solubility of methylcellulose-based edible films, *J. Food Eng.*, 2004, **61**(3), 459–466, DOI: **10.1016/S0260-8774(03)00155-9**.

25 P. Cazón, E. Morales-Sanchez, G. Velazquez and M. Vázquez, Measurement of the Water Vapor Permeability of Chitosan Films: A Laboratory Experiment on Food Packaging Materials, *J. Chem. Educ.*, 2022, **99**(6), 2403–2408, DOI: **10.1021/acs.jchemed.2c00449**.

26 A. Wexler, Vapor Pressure Formulation for Water in Range 0 to 100 °C. A Revision, *J. Res. Natl. Bur. Stand., Sect. A*, 1976, **80A**(5–6), 775–785, DOI: **10.6028/jres.080A.071**.

27 I. Y. Wu, S. Bala, N. Škalko-Basnet and M. P. di Cagno, Interpreting non-linear drug diffusion data: utilizing Korsmeyer-Peppas model to study drug release from liposomes, *Eur. J. Pharm. Sci.*, 2019, **138**, 105026, DOI: **10.1016/j.ejps.2019.105026**.

28 X. Zhai, M. Li, R. Zhang, W. Wang and H. Hou, Extrusion-blown starch/PBAT biodegradable active films incorporated with high retentions of tea polyphenols and the release kinetics into food simulants, *Int. J. Biol. Macromol.*, 2023, **227**, 851–862, DOI: **10.1016/j.ijbiomac.2022.12.194**.

29 L. L. Lao, S. S. Venkatraman and N. A. Peppas, Modeling of drug release from biodegradable polymer blends, *Eur. J. Pharm. Biopharm.*, 2008, **70**(3), 796–803, DOI: **10.1016/j.ejpb.2008.05.024**.

30 W. Brand-Williams, M. E. Cuvelier and C. Berset, Use of a free radical method to evaluate antioxidant activity, *LWT–Food Sci. Technol.*, 1995, **28**(1), 25–30, DOI: **10.1016/S0023-6438(95)80008-5**.

31 M. H. Romney, J. Ambler, L. M. Stephanie, M. Castanheira, T. Dingle, A. H. Janet, L. Koeth and K. Sei, CLSI Methods Development and Standardization Working Group Best Practices for Evaluation of Antimicrobial Susceptibility Tests, *J. Clin. Microbiol.*, 2018, **56**(4), DOI: **10.1128/jcm.01934-01917**.

32 J. I. Hedges and J. H. Stern, Carbon and nitrogen determinations of carbonate-containing solids, *Limnol. Oceanogr.*, 1984, **29**(3), 657–663, DOI: **10.4319/lo.1984.29.3.0657**.

33 H. Yu, Y. Ge, H. Ding, Y. Yan and L. Wang, Vanillin cross-linked chitosan/gelatin bio-polymer film with antioxidant, water resistance and ultraviolet-proof properties, *Int. J. Biol. Macromol.*, 2023, **253**, 126726, DOI: **10.1016/j.ijbiomac.2023.126726**.

34 B. A. Alimi, M. Hoque, S. Pathania, J. Wilson, B. Duffy and J. M. C. Frias, Structural, thermal, optical, and mechanical properties of composite films developed from the button mushroom (Agaricus bisporus)-sourced high molecular weight chitosan and potato starch, *LWT*, 2023, **185**, 115201, DOI: **10.1016/j.lwt.2023.115201**.

35 Z. Liu, X. Ge, Y. Lu, S. Dong, Y. Zhao and M. Zeng, Effects of chitosan molecular weight and degree of deacetylation on the properties of gelatine-based films, *Food Hydrocolloids*, 2012, **26**(1), 311–317, DOI: **10.1016/j.foodhyd.2011.06.008**.

36 W. Dai, L. Zhou, S. Gu, W. Wang, Z. Xu, X. Zhou and Y. Ding, Preparation and characterization of chitosan films incorporating epigallocatechin gallate: microstructure, physicochemical, and bioactive properties, *Int. J. Biol. Macromol.*, 2022, **211**, 729–740, DOI: **10.1016/j.ijbiomac.2022.04.226**.

37 S. Roy, R. Ramakrishnan, G. Goksen, S. Singh and Ł. Łopusiewicz, Recent progress on UV-light barrier food packaging films – a systematic review, *Innovative Food Sci. Emerging Technol.*, 2024, **91**, 103550, DOI: **10.1016/j.ifset.2023.103550**.

38 X. Zhang, Y. Li, M. Guo, T. Z. Jin, S. A. Arabi, Q. He, B. B. Ismail, Y. Hu and D. Liu, Antimicrobial and UV Blocking Properties of Composite Chitosan Films with

Curcumin Grafted Cellulose Nanofiber, *Food Hydrocolloids*, 2021, **112**, 106337, DOI: **10.1016/j.foodhyd.2020.106337**.

39 S. Bhowmik, D. Agyei and A. Ali, Enhancement of mechanical, barrier, and functional properties of chitosan film reinforced with glycerol, COS, and gallic acid for active food packaging, *Sustain. Mater. Technol.*, 2024, **41**, e01092, DOI: **10.1016/j.susmat.2024.e01092**.

40 J. Zhu, X. Chen, T. Huang and D. Tian, Comparative study on the characterization of chitosan mixed natural phenolic aldehyde edible films, *J. Appl. Polym. Sci.*, 2024, **141**(47), e56252, DOI: **10.1002/app.56252**.

41 Y. Peng, Y. Wu and Y. Li, Development of tea extracts and chitosan composite films for active packaging materials, *Int. J. Biol. Macromol.*, 2013, **59**, 282–289, DOI: **10.1016/j.ijbiomac.2013.04.019**.

42 J. Zhu, X. Chen, T. Huang, D. Tian and R. Gao, Characterization and antioxidant properties of chitosan/ethyl-vanillin edible films produced via Schiff-base reaction, *Food Sci. Biotechnol.*, 2023, **32**(2), 157–167, DOI: **10.1007/s10068-022-01178-w**.

43 E. Jakubowska, M. Gierszewska, J. Nowaczyk and E. Olewnik-Kruszkowska, Physicochemical and storage properties of chitosan-based films plasticized with deep eutectic solvent, *Food Hydrocolloids*, 2020, **108**, 106007, DOI: **10.1016/j.foodhyd.2020.106007**.

44 V. G. Bhat, S. S. Narasagoudr, S. P. Masti, R. B. Chougale, A. B. Vantamuri and D. Kasai, Development and evaluation of Moringa extract incorporated Chitosan/Guar gum/Poly(vinyl alcohol) active films for food packaging applications, *Int. J. Biol. Macromol.*, 2022, **200**, 50–60, DOI: **10.1016/j.ijbiomac.2021.12.116**.

45 G. G. Buonocore, A. Conte, M. R. Corbo, M. Sinigaglia and M. A. Del Nobile, Mono- and multilayer active films containing lysozyme as antimicrobial agent, *Innovative Food Sci. Emerging Technol.*, 2005, **6**(4), 459–464, DOI: **10.1016/j.ifset.2005.05.006**.

46 S. F. Hosseini, M. Zandi, M. Rezaei and F. Farahmandghavi, Two-step method for encapsulation of oregano essential oil in chitosan nanoparticles: preparation, characterization and in vitro release study, *Carbohydr. Polym.*, 2013, **95**(1), 50–56, DOI: **10.1016/j.carbpol.2013.02.031**.

47 W. L. Zhang, X. X. Li and W. B. Jiang, Development of antioxidant chitosan film with banana peels extract and its application as coating in maintaining the storage quality of apple, *Int. J. Biol. Macromol.*, 2020, **154**, 1205–1214, DOI: **10.1016/j.ijbiomac.2019.10.275**.

48 A. Lopez-Cordoba, C. Medina-Jaramillo, D. Pineros-Hernandez and S. Goyanes, Cassava starch films containing rosemary nanoparticles produced by solvent displacement method, *Food Hydrocolloids*, 2017, **71**, 26–34, DOI: **10.1016/j.foodhyd.2017.04.028**.

49 C. L. de Dicastillo, C. Nerín, P. Alfaro, R. Catalá, R. Gavara and P. Hernández-Muñoz, Development of New Antioxidant Active Packaging Films Based on Ethylene Vinyl Alcohol Copolymer (EVOH) and Green Tea Extract, *J. Agric. Food Chem.*, 2011, **59**(14), 7832–7840, DOI: **10.1021/jf201246g**.

50 R. Li, Z. Liu, J. Guo, W. Xu, X. Ning, X. Li, M. He and Q. Liu, Active chitosan films crosslinked by vanillin-derived dialdehyde for effective fruit preservation, *Food Hydrocolloids*, 2025, **164**, 111147, DOI: **10.1016/j.foodhyd.2025.111147**.

51 A. Oberlintner, M. Bajić, G. Kalčíková, B. Likozar and U. Novak, Biodegradability study of active chitosan biopolymer films enriched with Quercus polyphenol extract in different soil types, *Environ. Technol. Innovat.*, 2021, **21**, 101318, DOI: **10.1016/j.eti.2020.101318**.

52 B. Kaczmarek-Szczepańska, M. M. Sionkowska, O. Mazur, J. Świątczak and M. S. Brzezinska, The role of microorganisms in biodegradation of chitosan/tannic acid materials, *Int. J. Biol. Macromol.*, 2021, **184**, 584–592, DOI: **10.1016/j.ijbiomac.2021.06.133**.

53 B. K. H. Lim and E. S. Thian, Effects of molecular weight of chitosan in a blend with polycaprolactone and grapefruit seed extract for active packaging and biodegradation, *Food Packag. Shelf Life*, 2022, **34**, 100931, DOI: **10.1016/j.fpsl.2022.100931**.

54 N. Wrońska, N. Katir, M. Nowak-Lange, A. El Kadib and K. Lisowska, Biodegradable Chitosan-Based Films as an Alternative to Plastic Packaging, *Foods*, 2023, **12**(18), 3519.

55 C. Liu, H. Zhang, R. Xiao and S. Wu, Value-added organonitrogen chemicals evolution from the pyrolysis of chitin and chitosan, *Carbohydr. Polym.*, 2017, **156**, 118–124, DOI: **10.1016/j.carbpol.2016.09.024**.

56 S. Braccini, C.-B. Chen, J. J. Łucejko, F. Barsotti, C. Ferrario, G.-Q. Chen and D. Puppi, Additive manufacturing of wet-spun chitosan/hyaluronic acid scaffolds for biomedical applications, *Carbohydr. Polym.*, 2024, **329**, 121788, DOI: **10.1016/j.carbpol.2024.121788**.